A Conservative $k - \omega$ model for canonical shock-turbulence interaction

Krishnendu Sinha and S. J. Balasridhar
Department of Aerospace Engineering,
Indian Institute of Technology Bombay, Mumbai, 400076, India.

Abstract

Computation of shock-dominated turbulent flows using Reynolds-averaged turbulence models may encounter large numerical error. This is due to the fact that source terms in the turbulence model equations have nonconservative derivatives of mean flow quantities. The nonconservative error takes large values at flow discontinuities. In this paper, we study the numerical characteristics of the $k - \omega$ turbulence model in canonical interaction of a normal shock with homogeneous isotropic turbulence. Several cases with varying shock strength are computed, and the results are compared with exact solution. The effect of grid refinement is also reported. The governing equations are cast in an equivalent conservation form that gives physically consistent results at a shock wave. The predicted turbulence amplification match the exact solution obtained by direct integration of the simplified equations.

1. Introduction

Shock-boundary layer interactions are found in many aerospace applications. The Reynolds numbers are usually high such that the flow is turbulent. The shock wave formed on an airfoil at transonic speeds often results in boundary layer separation that affects the aerodynamic performance. Shock waves formed in hypersonic intakes of scramjet engines can cause localized high pressure and heat transfer. Separation bubbles formed due to shock-boundary layer interaction inside the duct can lead to intake unstart. The interaction of turbulent fluctuations in the boundary layer with the shock wave lies at the heart of these phenomena. Shock-turbulence interaction has therefore been the focus of several studies.

Homogeneous isotropic turbulence passing through a normal shock is possibly the simplest shock-turbulence interaction. The upstream mean flow is uniform in space and time, and therefore does not have additional mean flow gradients like in boundary layers. Flow separation characteristic of strong shock-boundary layer interactions is absent. Additional complexity due to oblique and curved shock waves, free shear layers, reattachment and recovery of the boundary layer are also eliminated. The canonical shock-homogeneous turbulence interaction therefore isolates the effect of the shock wave on the turbulent fluctuations.

Shock-homogeneous turbulence interaction has been studied using theoretical, computational and experimental approaches. Theoretical analysis using rapid distortion theory [1, 2] and linear interaction analysis [3, 4] are based on the assumption that the mean flow distortion is much faster than the turbulent time scales. Full three-dimensional Navier-Stokes simulations of these flows are reported in [5–8], among others. Experimenal results of Barre et al [9] complement the numerical studies. Shock-homoegeneous turbulence interaction is rich in physics and it provides valuable insight that has been used for turbulence model development [10–12]. The model problem also serves as a good test case for numerical studies, as shown in Ref. [13].

Turbulent kinetic energy (TKE) variation in a shock-homogeneous turbulence interaction, as obtained in direct numerical simulation, is shown in Fig. 1, reproduced from Ref. 12. A normal shock wave with an upstream Mach number of 1.5 is located at $x = 3$. In the absence of any mean flow gradient, the turbulent fluctuations decay in the upstream flow. The decay rate is determined by the turbulent dissipation rate. The shock wave amplifies the turbulent fluctuations, followed by a monotonic decay governed by the downstream dissipation rate. High levels of TKE are reported in the vicinity of the shock wave, but these do not represent turbulent fluctuations.

Computations using Reynolds-averaged Navier Stokes (RANS) method are also shown for comparison. The numerical results follow the DNS data qualitatively, but the amplification of turbulence predicted at the shock wave varies for different turbulence models. Three representative models – standard $k - \epsilon$, a realizable $k - \epsilon$ and a recent model based on unsteady shock motion – are plotted. It is shown that TKE amplification is often over-predicted by RANS turbulence models. This is because of the highly non-equilibrium nature of the interaction, and subsequent breakdown of the assumptions underlying the turbulence model equations.

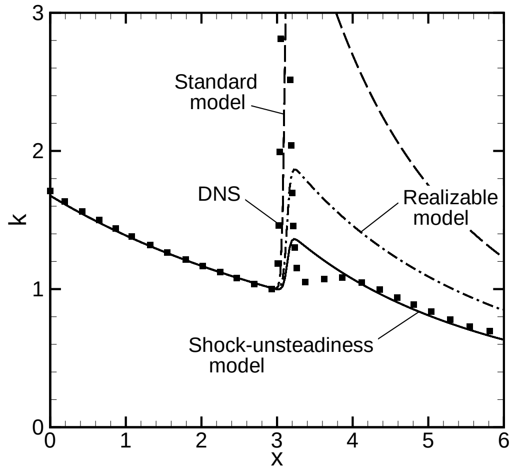

Figure 1: Evolution of turbulent kinetic energy in homogeneous isotropic turbulence passing through a Mach 1.5 normal shock. Different versions of the $k-\epsilon$ model are compared with DNS data. [7]

RANS simulations can result in large numerical error at flow discontinuities like shock waves. It is shown in Ref. [13] that the source terms contain non-conservative derivatives of the flow variables, and the corresponding discretization error attain large values in a flow discontinuity. Further, the error does not decrease with successive grid refinement. It is also found that there is excessive amplification of the turbulent dissipation rate at high Mach numbers, which can cause rapid decay of the downstream turbulence.

In this paper, we study the numerical characteristics of the $k-\omega$ turbulence model for canonical shock/turbulence interaction. A finite-volume based CFD code is used for the simulations. The evolution of k and ω across the normal shock wave is presented for a range of upstream mean flow Mach numbers. Effect of grid refinement on the turbulence amplification at the shock is quantified, and is compared with exact closed-form solution of the governing equations. An alternate conservative form of the $k-\omega$ equations are derived and implemented in the finite-volume code. The advantages of the new formulation over the traditional non-conservative $k-\omega$ equations is presented for the chosen test cases.

2. Governing Equations

The equations governing the turbulence kinetic energy k and specific dissipation rate ω are given by [14]

$$\frac{\partial(\rho k)}{\partial t}+\frac{\partial(\rho u_j k)}{\partial x_j}=\rho\tau_{ij}\frac{\partial u_i}{\partial x_j}-\beta^*\rho k\omega+\frac{\partial}{\partial x_j}\left[\left(\mu+\sigma^*\frac{\rho k}{\omega}\right)\frac{\partial k}{\partial x_j}\right] \tag{1}$$

$$\frac{\partial(\rho\omega)}{\partial t}+\frac{\partial(\rho u_j\omega)}{\partial x_j}=\alpha\frac{\omega}{k}\rho\tau_{ij}\frac{\partial u_i}{\partial x_j}-\beta\rho\omega^2+\sigma_d\frac{\rho}{\omega}\frac{\partial k}{\partial x_j}\frac{\partial\omega}{\partial x_j}+\frac{\partial}{\partial x_j}\left[\left(\mu+\sigma\frac{\rho k}{\omega}\right)\frac{\partial k}{\partial x_j}\right] \tag{2}$$

where ρ is mean density, u_j is the mean velocity in x_j direction and μ is molecular viscosity. The Reynolds stress tensor is given by

$$\rho\tau_{ij}=2\mu_T\overline{S}_{ij}-\frac{2}{3}\rho k\delta_{ij} \quad \text{where} \quad \overline{S}_{ij}=S_{ij}-\frac{1}{3}\frac{\partial u_k}{\partial x_k}\delta_{ij} \tag{3}$$

and the eddy viscosity is

$$\mu_T=\frac{\rho k}{\tilde{\omega}}, \qquad \tilde{\omega}=max\left\{\omega,\, C_{lim}\sqrt{\frac{2\overline{S}_{ij}\overline{S}_{ij}}{\beta^*}}\right\} \tag{4}$$

The closure coefficients are $\beta^*=9/100$ and

$$\beta=\beta_o f_\beta, \qquad \beta_o=0.0708, \qquad f_\beta=\frac{1+85\chi_\omega}{1+100\chi_\omega} \tag{5}$$

where

$$\chi_\omega = \left|\frac{\Omega_{ij}\Omega_{jk}\hat{S}_{ki}}{(\beta^*\omega)^3}\right|, \qquad \hat{S}_{ki} = S_{ki} - \frac{1}{2}\frac{\partial u_m}{\partial x_m}\delta_{ki} \tag{6}$$

In the canonical shock turbulence interaction considered in this work, the vorticity tensor Ω_{jk} is identically zero, which yields $\chi_\omega = 0$ and $\beta = \beta_0$.

The mean flow through a normal shock is one-dimensional and steady, with a mean velocity u in the x direction. The production terms on the right hand side are proportional to the mean-flow gradient at the shock. They have a dominant effect in amplifying turbulence across the shock wave. The dissipation terms determine the rate of decay in the upstream and downstream flows. The turbulent and molecular diffusion effects are small, and are neglected. The resulting $k-\omega$ equations can be written as

$$\rho u\frac{\partial k}{\partial x} = -1.15\rho k\frac{\partial u}{\partial x} - \beta^*\rho k\omega\,, \tag{7}$$

$$\rho u\frac{\partial \omega}{\partial x} = -0.598\rho\omega\frac{\partial u}{\partial x} - \beta\rho\omega^2\,, \tag{8}$$

Neglecting dissipation, and integrating the resulting equations analytically yields the following amplification in k and ω in terms of the mean density ratio across the shock wave.

$$\frac{k_2}{k_1} = \left(\frac{\rho_2}{\rho_1}\right)^{1.15} \text{ and } \quad \frac{\omega_2}{\omega_1} = \left(\frac{\rho_2}{\rho_1}\right)^{0.598} \tag{9}$$

The above closed-form solutions are used for comparison with numerical results.

3. Simulation Results

The Reynolds-averaged Navier Stokes equations are solved for the mean flow, and the two-equation $k-\omega$ model is used for turbulence closure. The flow variables are normalized by the mean density and mean speed of sound upstream of the shock wave. The most energetic wave number κ_0 in the incoming turbulence field is taken as the characteristic length scale. A finite-volume approach is used, where the turbulence model equations are fully coupled with the mean flow conservation equations [15]. The inviscid fluxes are computed with a modified, low-dissipation form of the Steger-Warming flux-vector splitting method [16].

The viscous fluxes due to molecular and turbulent diffusivities are computed using a second-order central difference method applied at each cell face. The turbulent source terms are evaluated at the cell centers, where the velocity gradients in the production terms are discretized using a central difference scheme akin to that presented in Appendix. The implicit data parallel line relaxation method of Wright *et al.* [17] is employed for time integration and the code has been used successfully in several supersonic and hypersonic applications. Some representative results are presented in Refs. 18, 19 and 20.

The canonical shock-turbulence interaction flows considered in this work are listed in Table 1. The turbulent Mach number immediately upstream of the shock wave is 0.22 and the Reynolds number based on Taylor microscale is 40 at this location [8]. The normalized values of TKE and specific dissipation rate are thus calculated and are extrapolated to the inlet station using the decay relations for homogeneous isotropic turbulence. These values are listed in Table 1 and are specified at the inlet location. Additional details of the simulation can be found in [13].

Table 1: Mean and turbulent flow quantities for the interaction of homogeneous turbulence with a normal shock. The normalized values of k and ω correspond to the inflow station.

M	k_0	ω_0	DNS Source
1.5	2.88×10^{-2}	0.436	Larsson and Lele [8]
2.0	2.76×10^{-2}	0.431	—
2.5	2.69×10^{-2}	0.428	Larsson and Lele [8]
3.0	2.64×10^{-2}	0.427	—
3.5	2.61×10^{-2}	0.426	Larsson and Lele [8]
4.25	2.57×10^{-2}	0.426	—

Figure 2 plots the jump in k and ω across the shock as a function of the upstream mean flow Mach number. The finite-volume computations for the chosen test cases are compared with the close-form solution of the $k-\omega$ equations.

For weak shocks (for example, $M = 1.5$ case), the predictions are comparable to the exact solution, but the simulations over-predict k and ω-amplification for higher Mach numbers. For the strongest shock simulated in this work, the post-shock tubulent kinetic energy deviates from the exact solution by over an order in magnitude. The amplification of ω show a similar trend, but the values are relatively closer to the exact integration.

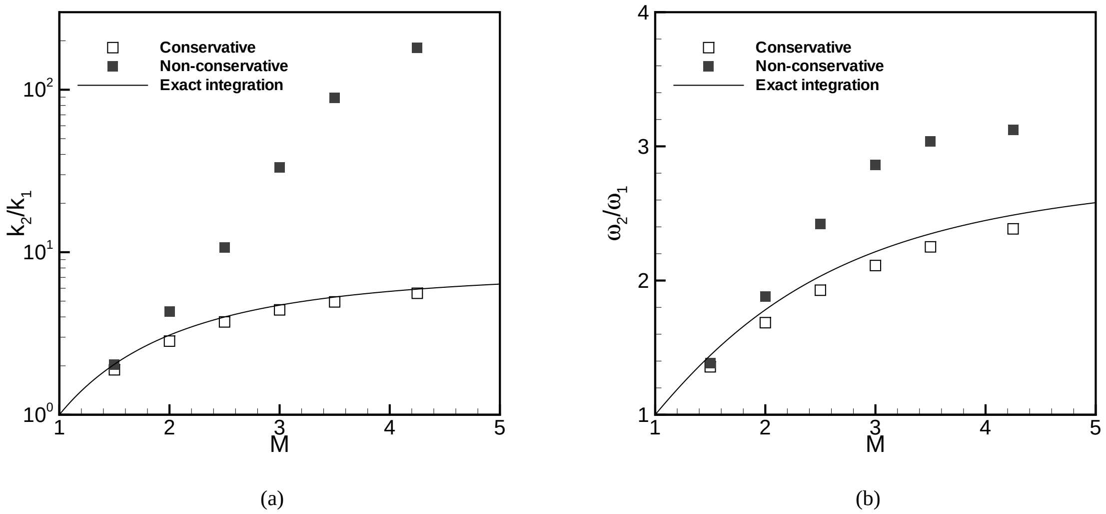

Figure 2: Variation in k- and ω-amplification with upstream Mach number as computed using the conservative and non-conservative formulations.

4. Conservative Formulation

Noting that $k \propto \rho^{1.15}$ across the shock wave in the inviscid limit, we define a new variable $f = k\rho^{-1.15}$ that is constant across a shock. A transport equation for f can be derived by multiplying (7) by $\rho^{-1.15}$

$$\rho^{-1.15}\,\rho u\frac{\partial k}{\partial x} = -1.15\rho k\frac{\partial u}{\partial x}\rho^{-1.15} - \beta^{*}\rho k\omega\rho^{-1.15}\,. \tag{10}$$

Mass conservation across the shock wave is used to write

$$\rho uk\frac{\partial}{\partial x}\rho^{-1.15} = 1.15\rho k\frac{\partial u}{\partial x}\rho^{-1.15}\,. \tag{11}$$

Adding (10) and (11), we get

$$\rho u\frac{\partial f}{\partial x} = -\beta^{*}\rho k\omega\rho^{-1.15}\,, \tag{12}$$

where the source term with non-conservative derivative is eliminated. Similar development for the ω-equation leads to a new variable, $g = \omega\rho^{-0.598}$ and the corresponding transport equation is

$$\rho u\frac{\partial g}{\partial x} = -\beta\rho\omega^{2}\,\rho^{-0.598}. \tag{13}$$

Substituting $\omega = g\rho^{0.598}$ and $k = f\rho^{1.15}$, the above equations can be cast into the following form:

$$\rho u\frac{\partial f}{\partial x} = -\beta^{*}\rho f g\,\rho^{0.598}, \tag{14}$$

$$\rho u\frac{\partial g}{\partial x} = -\beta\rho g^{2}\,\rho^{0.598}, \tag{15}$$

which are similar to the original equations (7) and (8), except for the absence of the production terms. The dissipation terms retain their original form with an additional factor of $\rho^{0.598}$.

The finite-volume code is based on the turbulence model equations (1) and (2). The new form of the model equations suitable for shock-dominated flows can be incorporated by [13] :

1. interpreting the turbulence variables in the code as f and g, instead of k and ω.

2. transforming the initial and boundary conditions for k and ω to the new variables f and g.

3. dropping the production terms in each equation and multiplying the dissipation terms by a factor $\rho^{0.598}$.

4. recovering the original turbulence variables k and ϵ from the converged flowfield solution by invoking the reverse transforms.

The TKE and specific dissipation rate amplification obtained using the new conservative form of the turbulence model equations are plotted in Fig. 2. The results follow the exact solution closely, both in terms of qualitative and quantitative comparison. Both k and ω predictions are lower than the inviscid limit (9), because of the effect of turbulent dissipation in the shock region. The dissipation effect is neglected while integrating the respective production terms to arrive at (9).

5. Grid Sensitivity

The sensitivity of the numerical results to the grid-point density used in the computation are presented in this section. The results obtained by the new conservative and the conventional non-conservative forms of the turbulence model are compared with the exact solution. Two equi-spaced grids with successive refinement (200 and 400 points in the shock-normal direction) are employed, and the amplifications of TKE and specific dissipation rate plotted as a function of the shock strength.

In the conservative case, both k and ω amplifications approach the exact inviscid solution as the grid is refined (see Fig. 3). As shown in [13], the discretization error in the convection terms decrease as Δx^2), where Δx is grid spacing at the shock wave. The damping effect of turbulent dissipation at the shock scales as Δx, and it also decreases as the shock gets thinner. Thus, the numerical solution approaches the exact inviscid integration (9) as $\Delta x \to 0$ on fine grids.

The turbulence amplification predicted by the non-conservative turbulence model equations (see Fig. 4) show marginal increase as the grid is refined. The increase in the post-shock k and ω takes the solution away from the exact integration values. Interestingly, the non-conservative $k-\epsilon$ model results presented in [13] shows much higher sensitivity to the grid-point density. The amplification in turbulent dissipation rate is found to increase dramatically as the grid is refined in the vicinity of the shock wave. See Fig. 8(b) in [13].

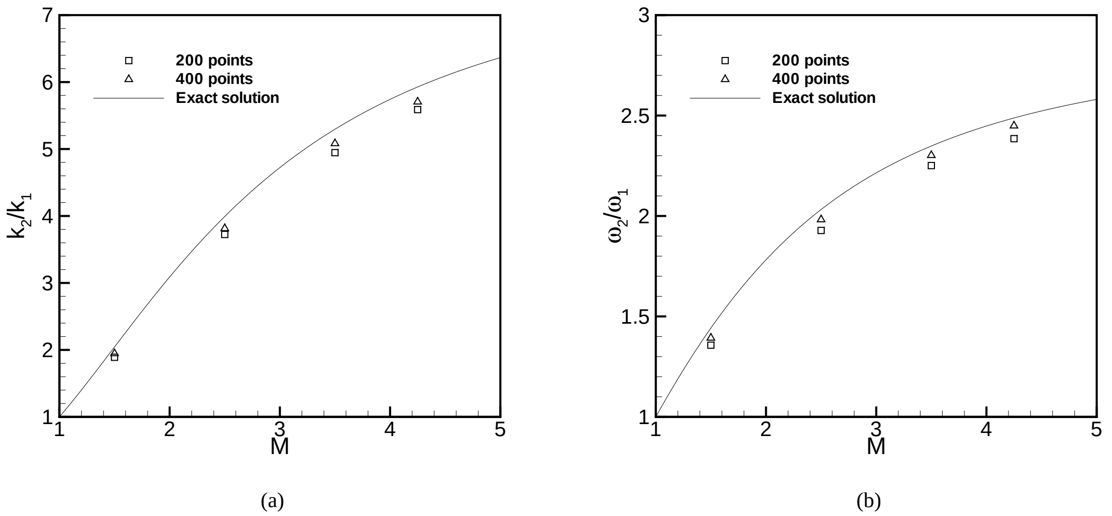

Figure 3: Amplification in TKE and specific dissipation rate across a shock wave as a function of upstream Mach number for varying grid-point density, obtained using the conservative $k-\omega$ equations.

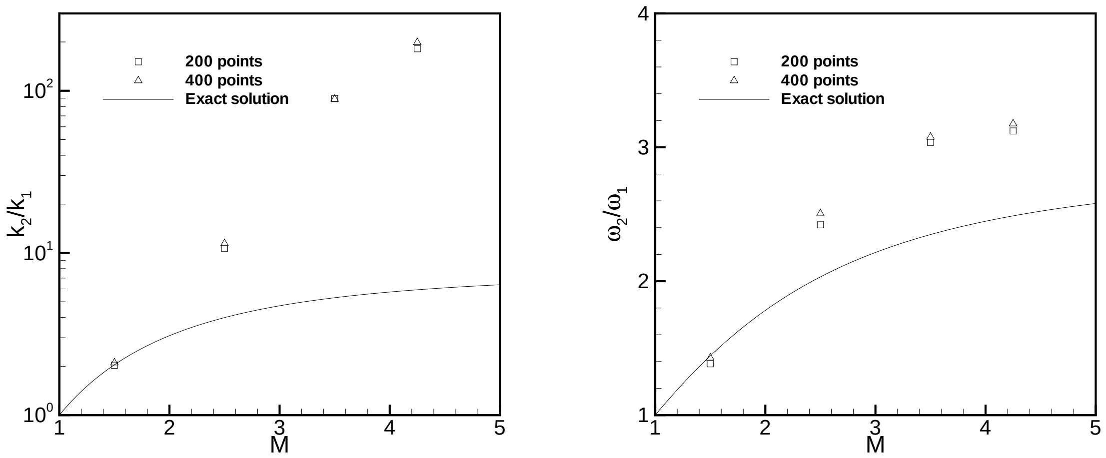

(a) (b)

Figure 4: Amplification in TKE and specific dissipation rate across a shock wave as a function of upstream Mach number for varying grid-point density, obtained using the non-conservative $k - \omega$ equations.

6. Conclusions

In this paper, we investigate the numerical characteristics of Reynolds-averaged Navier Stokes simulations at a shock wave. The $k - \omega$ turbulence model equations have non-conservative source terms, which result in large error in the region of the shock. The non-conservative errors do not vanish on successive grid refinement, leading to non-physical behavior of the numerical solution. An alternate conservative formulation of the $k - \omega$ equations is proposed which eliminates the non-conservative source terms. The resulting equations yield well-bahaved solution at shock waves that match the exact solution closely.

References

[1] Durbin, P. A., and Zeman, O. 1992. Rapid Distortion Theory for Homogeneous Compressed Turbulence with Application to Modelling. *Journal of Fluid Mechanics*. 242:349–370

[2] Cambon, C., Coleman, G. N., and Mansour, N. N. 1993. Rapid Distortion Analysis and Direct Simulation of Compressible Homogeneous Turbulence at Finite Mach Number. *Journal of Fluid Mechanics*. 257:641–641

[3] Mahesh, K., Moin, P., and Lele, S. K. 1996. The Interaction of a Shock Wave with a Turbulent Shear Flow. *AFOSR Report No. TF-69*. Thermosciences Division, Department of Mechanical Engineering, Stanford University, CA

[4] Wouchuk, J., Huete Ruiz de Lira, C., and Velikovich, A. 2009. Analytical Linear Theory for the Interaction of a Planar Shock Wave with an Isotropic Turbulent Vorticity Field. *Physical Review E*. 79:6

[5] Lee, S., Lele, S. K. and Moin, P. 1993. Direct numerical simulation of isotropic turbulence interacting with a weak shock wave. *Journal of Fluid Mechanics*. 251:533–562

[6] Mahesh, K., Lele, S. K., and Moin, P. 1997. The Influence of Entropy Fluctuations on the Interaction of Turbulence with a Shock Wave. *Journal of Fluid Mechanics*. 334:353–379

[7] Jamme, S., Cazalbou, J. B., Torres, F. and Chassaing, P. 2002. Direct numerical simulation of the interaction between a shock wave and various types of isotropic turbulence. *Flow, Turb. and Combust.*. 68:227–268

[8] Larsson, J. and Lele, S. K. 2009. Direct numerical simulation of canonical shock/turbulence interaction. *Physics of Fluids*. 21:126101

[9] Barre, S., Alem, D., and Bonnet, J. P. 1996. Experimental Study of a Normal Shock/Homogeneous Turbulence Interaction. *AIAA Journal*. 34:968–974.

[10] Sinha, K., Mahesh, K., and Candler, G. V. 2003. Modeling Shock-Unsteadiness in Shock/Turbulence Interaction. *Physics of Fluids*. 15:2290–2297.

[11] Veera, V. K., and Sinha, K. 2009. Modeling the Effect of Upstream Temperature Fluctuations on Shock/homogeneous Turbulence Interaction. *Physics of Fluids*. 21:025101

[12] Sinha, K. 2012. Evolution of Enstrophy in Shock/Homogeneous Turbulence Interaction. *Journal of Fluid Mechanics*. 707:74–110.

[13] Sinha, K., and Balasridhar, S.J. 2013. Conservative Formulation of the $k - \epsilon$ Turbulence Model for Shock-Turbulence Interaction. *AIAA Journal*. Early Edition.

[14] Wilcox, D. C., 2008. Formulation of the $k - \omega$ Turbulence Model Revisited. *AIAA Journal*. 46:11. 2823–2838.

[15] Sinha, K., and Candler, G. V. 1998. Convergence Improvement of Two-equation Turbulence Model Calculations. *AIAA Paper* 1998-2649.

[16] MacCormack, R. W. & Candler, G. V. 1989. The solution of the Navier-Stokes equations using Gauss Seidel line relaxation. *Computers and Fluids* 17:1, 135–150.

[17] Wright, M. J., Candler, G. V., and Bose, D. 1998. Data-Parallel Line Relaxation Method for the Navier-Stokes Equations. *AIAA Journal*. 36:9. 1603–1609.

[18] Sinha, K., Mahesh, K. and Candler, G. V. 2005. Modeling the effect of shock unsteadiness in shock/turbulent boundary layer interactions. *AIAA Journal*. 43:3, 586–594.

[19] Pasha, A. A. and Sinha, K. 2012 Simulation of hypersonic shock/turbulent boundary-layer interactions using shock-unsteadiness model. *Journal of Prop and Power*. 28:1, 46–60.

[20] Pasha, A. A. & Sinha, K. 2008. Shock-unsteadiness model applied to oblique shock-wave/ turbulent boundary layer interaction. *Int. J. Comput. Fluid Dyn.* 22:8, 569–582.